Statistical Mechanics of the Glass Transition in One-Component Liquids with an Anisotropic Potential

Valery Ilyin, Edan Lerner, Ting-Shek Lo, and Itamar Procaccia

Department of Chemical Physics, The Weizmann Institute of Science, Rehovot 76100, Israel

(Received 7 May 2007; published 28 September 2007)

We study a recently introduced model of one-component glass-forming liquids whose constituents interact with an anisotropic potential. This system is interesting per se and as a model of liquids such as glycerol (interacting via hydrogen bonds) which are excellent glass formers. We work out the statistical mechanics of this system, encoding the liquid and glass disorder using appropriate quasiparticles (36 of them). The theory provides a full explanation of the glass transition phenomenology, including the identification of a diverging length scale and a relation between the structural changes and the diverging relaxation times.

DOI: 10.1103/PhysRevLett.99.135702 PACS numbers: 64.70.Pf, 05.45.Df, 05.70.Fh, 61.43.Hv

The study of associated liquids such as glycerol as glass formers has a long and rich history [1], but until now the role of the anisotropic hydrogen bonds, while clearly important in frustrating crystallization, has not been made explicit. Recently, a model of one-component liquids with an anisotropic interaction potential was introduced [2], together with numerical simulations in two dimensions that demonstrated clearly the importance of the anisotropic interaction in frustrating crystallization and allowing the formation of a glassy state of matter. This model is important in stressing the fact that even simple one-component liquids may not crystallize if the local symmetry of the interaction potential does not perfectly match the symmetry of the equilibrium crystal. It is worthwhile, therefore, to analyze further this example of glass formation and put it in the general context of the glass transition. In this Letter, we present a theory of this model, constructing its statistical mechanics and providing an understanding of the phenomenology of its glass transition, including an identification of a diverging length and explaining the diverging time scales. Our analysis allows putting this interesting example of glass formation on the same footing as other classical glass formers such as binary mixtures with central potentials [3,4], stressing the generality of the approach [5,6] and of the glass transition phenomenon at the same time.

Particles of mass m in this model interact via

$$U(r_{ij}, \theta_i, \theta_j) = \bar{U}(r_{ij}) + \Delta U(r_{ij}, \theta_i, \theta_j), \tag{1}$$

where r_{ij} is the distance between the two particles i and j. The first term on the right-hand side of (1) is the standard isotropic Lennard-Jones potential

$$\bar{U}_{ij} = 4\epsilon\left[\left(\frac{\sigma}{r_{ij}}\right)^{12} - \left(\frac{\sigma}{r_{ij}}\right)^{6}\right], \tag{2}$$

whereas the anisotropic part of the potential is given by

$$\begin{aligned} \Delta U(r_{ij}, \theta_i, \theta_j) &= -4\epsilon\Delta\left(\frac{\sigma}{r_{ij}}\right)^{6}\left[h\left(\frac{\theta_i - \theta_0}{\theta_c}\right) + h\left(\frac{\theta_j - \theta_0}{\theta_c}\right) - \frac{64}{35\pi}\theta_c\right], \\ h(x) &= (1 - x^2)^3 \quad \text{for } |x| < 1; \\ h(x) &= 0 \quad \text{for } |x| \geq 1. \end{aligned} \tag{3}$$

Here θ_i (θ_j) is the included angle between the relative vector $\boldsymbol{r}_{ij} \equiv \boldsymbol{r}_i - \boldsymbol{r}_j$ and a unit vector $\boldsymbol{u}_i$ ($\boldsymbol{u}_j$) (referred to below as "spin") which represents the orientation of the axis of particle i (j). The function $h((\theta - \theta_0)/\theta_c)$ (with $\theta_0 = 126°$ and $\theta_c = 53.1°$) has a maximum at $\theta = \theta_0$, and thus θ_0 is a favored value of θ_i. Thus, the anisotropic term in the potential favors structures of fivefold symmetry. The parameter Δ controls the tendency of fivefold symmetry and, therefore, of the frustration against crystallization. The units of mass, length, time, and temperature are m, σ, $\tau = \sigma\sqrt{m/\epsilon}$, and ϵ/k_B, respectively, with k_B being Boltzmann's constant.

According to the numerical simulations presented in Ref. [2], for $\Delta < 0.6$ this system crystallizes upon reducing the temperature. The ground state crystal has an elongated hexagonal structure with antiferromagnetic ordering of the spins $\boldsymbol{u}_i$, but the actual crystal that is obtained upon cooling is a "plastic crystal" with hexagonal spatial order but with spin disorder. For $\Delta > 0.6$ the system fails to crystallize upon cooling. The relaxation times were measured by monitoring the rotational autocorrelation functions $C_R(t) \equiv (1/N)\sum_i\langle\boldsymbol{u}_i(t) \cdot \boldsymbol{u}_i(0)\rangle$, which was fitted to a stretched exponential form $C_R(t) \propto \exp[-(t/\tau_\alpha)^\beta]$. For $\Delta = 0.6$ the relaxation is of Arrhenius form with a constant value $\beta \approx 0.95$ for $T > T_m = 0.46$, but β was fit separately for every temperature $T < T_m$, where it decreases with temperature. The relaxation times were fitted to a Vogel-Fulcher law $\tau_\alpha = \tau_0 \exp[DT_0/(T - T_0)]$, which involves fitting the three free parameters $\tau_0 = 0.61$, $D = 7.4$, and $T_0 = 0.099$ (in addition to β). We repeated the simulations of this model using Monte Carlo methods in *N-P-T* ensemble [7], finding results in agreement with the molecular dynamics simulations of Ref. [2] in the same ensemble.

To construct the statistical mechanics of this system, we recognize that the potential energy between any pair of particles depends on their spin orientations. In Fig. 1, we present the three potentials between two particles, depending on the orientation of their spins relative to the interparticle vector distance: Lowest in energy (continuous blue line) is the case for which both have a favored spin orientation, and the middle (dashed green line) [respectively, high (dotted red line)] is the potential when one (respectively, none) of the spins is in a favored orientation. One sees that the minima of these potentials occur with significant gaps in their energies, allowing us to now measure the *average* energy of *pairs* of particles as a function of temperature. These averages fall in three distinct ranges, such that the range of variation of each energy is much smaller than the gaps between the energies; see the inset in Fig. 1. This allows us to proceed to define quasispecies. We denote the three effective energies below as $2E_b$, $2E_g$, and $2E_r$, respectively. Note that the spin orientations involved in each such mean energy can fluctuate within a temperature-dependent range of angles. For the temperature range of interest, the range of angles is in a sector of about 60°, but, as this range of angles determines the degeneracies that enter the statistical mechanics below, we need to reconsider it carefully as explained in the following. Next, consider an n star, which by definition is a given particle decorated by the n interparticle vector distances (edges) to its n neighbors; see, for example, Fig. 2. Each such edge is colored according to the spin orientations. We denote by i, j, and k the number of red, green, and blue edges, respectively, such that $n = i + j + k$. It turns out that, in the temperature range of interest ($0 < T < 0.5$), in an overwhelming majority of n stars (more than 98%), the central particle has a spin orientation that is favorable with respect to two of its edges (this is, of course, the maximal value, which is favored by energy considerations). Therefore, we take *a priori* $j + k \geq 2$, neglecting the very small number of instances where this does not hold. The energy of such an n star (referred to as a quasiparticle) is computed as

$$E_{ijk} = iE_r + jE_g + kE_b, \tag{4}$$

where $k \leq 2$. Note that, since the energies on the right-hand side of Eq. (4) depend on temperature, so does the energy of the quasiparticles. Notwithstanding, in the interesting temperature range the temperature dependence is weak; we take the energies of the quasiparticles as T-independent (we used half the energy of a particle pair $E_r = -0.2187$, $E_g = -0.5645$, $E_b = -1.5105$). The degeneracy g_{ijk} of the energy level (number of quasiparticles with the same energy) is

$$g_{ijk} = \binom{2}{k}\binom{i+j+k-2}{i} 2^{j+2k-2} 4^{i-k+2}. \tag{5}$$

Since the central particle always has a spin in favorable orientation to two edges, each of these two edges must be blue or green; the first factorial is the number of possible choices of blue edges, one way if there are two (or none) of them and two ways if there is one of them. Once these two edges are determined, there remain $i + j + k - 2$ edges to choose the i red from, giving rise to the second factorial. This completes the degeneracy due to color. Next, we count the number of spin orientations. There are $2 - k$

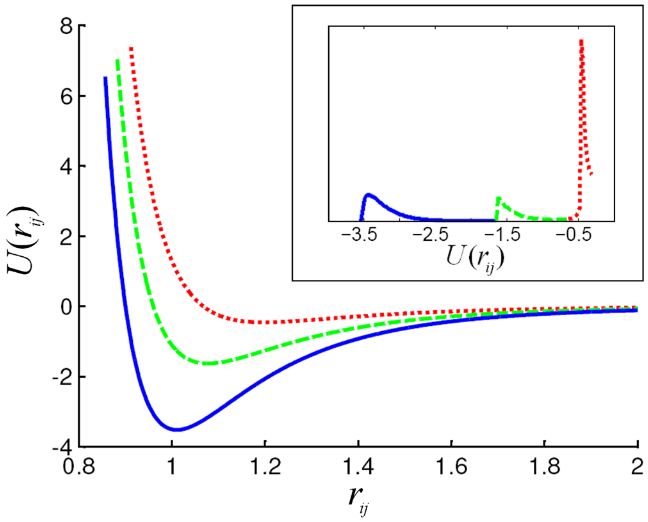

FIG. 1 (color online). Potential curves for particle pairs with two spins, one spin, or no spin in the favored position (continuous blue line, dashed green line, or dotted red line, respectively). Inset: The measured energies of particle pairs, falling in three distinct ranges with gaps between them, allowing us to define the quasiparticles. The peak in each colored curve corresponds to the minimum in the main figure.

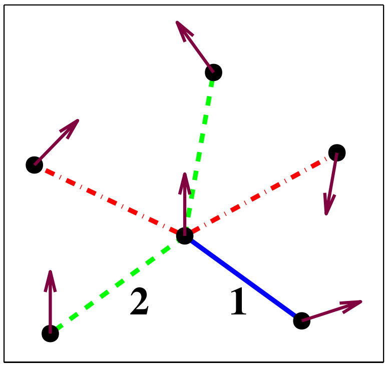

FIG. 2 (color online). An example of an n star with $n = 5$, $i = 2$, $j = 2$, and $k = 1$. The central particle has a spin with the favored orientation with respect to edges 1 and 2. Thus, these edges can be either blue or green, and this central spin cannot be favored with respect to any other edge. In the interesting range of temperatures, we observe 36 n stars with $4 \leq i + j + k \leq 6$.

green edges due to the central particle and i red edges, giving us $i - k + 2$ unfavorable spin orientations and $j + 2k - 2$ favorable ones. The number of ways to orient the unfavorable spins is 4^{i-k+2}, and the number of ways to orient the favorable spins is 2^{j+2k-2}. The number 4 stems from the fact that the two favored orientations occupy an angular sector of $2 \times 60°$, leaving us with 4 sectors of 60° for the unfavorable orientations. The fact that the central particle can emanate at most two favored edges means that we have a constraint $\sum_{ijk}(j + 2k)c_{ijk} \leq 4$, where c_{ijk} is the mol fraction of quasiparticles having i, j, and k edges of the right color. In practice, as mentioned above, the inequality can be swapped with an equality

$$\sum_{ijk}(j + 2k)c_{ijk} = 4. \tag{6}$$

To satisfy this constraint exactly, we need to consider the temperature dependence of the spin-fluctuation sectors, since when these change, so do the assignments of (ijk). In Fig. 3, we show the left-hand side of Eq. (6) for two fixed spin-fluctuation sectors [upper, red squares, 69°; lower, green diamonds, 50°; middle, blue circles, variable sector of width $w = (68.5T + 41.2)°$]. In all cases, the sum was measured via Monte Carlo simulations in the range $0.05 < T < 0.5$. The quality of the constraint using the variable spin-fluctuation sector is obvious. The decrease at high temperatures is due to the increased fluctuations in the spin orientations and in the energies of the quasiparticles, inducing changes in the degeneracies and in the (ijk) assignments. We thus use this temperature-dependent width of the spin fluctuations to assign the quasiparticle index (ijk) in all our simulations.

Now write the partition function of the system:

$$Z(T, \lambda(T)) \equiv \sum_{ijk} g_{ijk} e^{-\beta E_{ijk}} e^{-\lambda(j+2k)}. \tag{7}$$

The Lagrange multiplier λ is introduced to ensure that the constraint (6) is satisfied. In terms of the partition function, the mol fraction of quasiparticles is

$$c_{ijk} = \frac{g_{ijk} e^{-\beta E_{ijk}} e^{-\lambda(j+2k)}}{Z(T, \lambda(T))}. \tag{8}$$

Substituting Eq. (8) in Eq. (6), we compute $\lambda(T)$ for each temperature and then compute the mol fraction c_{ijk}. For presentation and comparison with numerical simulations, it is advantageous to bunch groups of c_{ijk} together. One bunching is in the three groups obtained with $k = 0, 1, 2$. In Fig. 4, we present a comparison of the theory to the simulation for the mol fractions of quasiparticles with $k = 0, 1, 2$. We note that the agreement is excellent down to $T \approx 0.17$, where the simulation gets jammed. This observation is in agreement with Ref. [2], where it was estimated that the glass transition temperature is about 0.15 on the basis of the "divergence" of relaxation times. We note that the statistical mechanics predicts the precise spin statistics of the glassy jammed state, since the mol fractions freeze at a "fictive temperature" $T \approx 0.17$ that can be read directly from Fig. 4. We do not need to measure relaxation times to see where the system falls out of equilibrium; it is obvious directly from Fig. 4.

In addition, the statistical mechanics predicts two "transitions" when the mol fractions of quasispecies with $k = 0$ and then with $k = 1$ become small. The glass transition (jamming) occurs visibly when the mol fraction $c_{k=0}$ becomes small. We read a second transition when $c_{k=1}$ becomes exponentially small. This implies that the ground state consists solely of $k = 2$ quasiparticles, in perfect agreement with the existence of the a crystalline ground

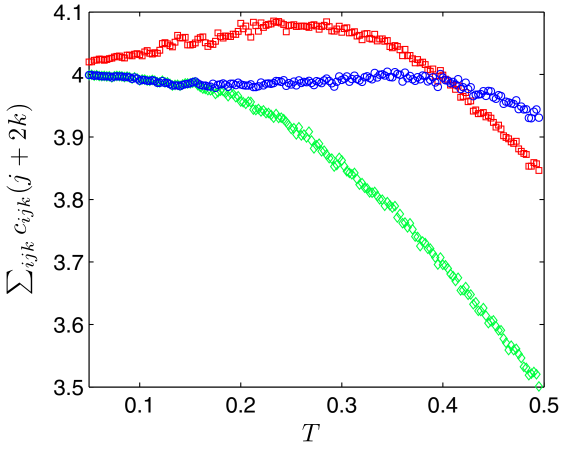

FIG. 3 (color online). Direct numerical simulation of the constraint (6).

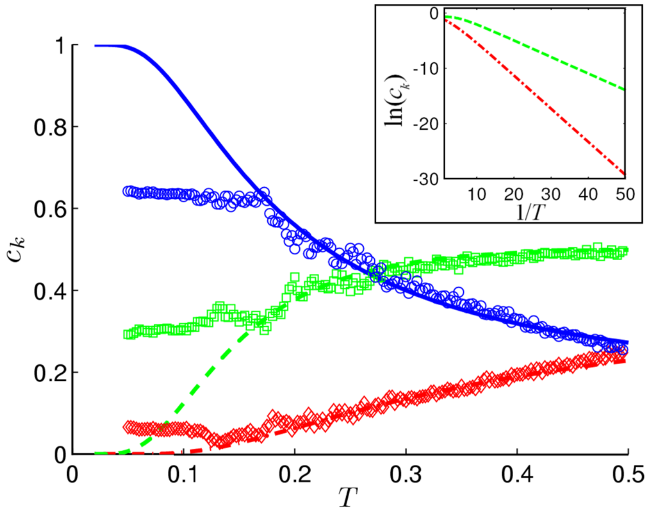

FIG. 4 (color online). Comparison of the direct numerical simulations to the theoretical prediction. Shown are the mol fractions c_k, with $k = 0$ (dashed-dotted red line), $k = 1$ (dashed green line), and $k = 2$ (continuous blue line). One sees the point of departure of the direct numerical simulations from equilibrium (the point of jamming) which is estimated to be about $T = 0.17$. Inset: The same concentrations on a logarithmic scale.

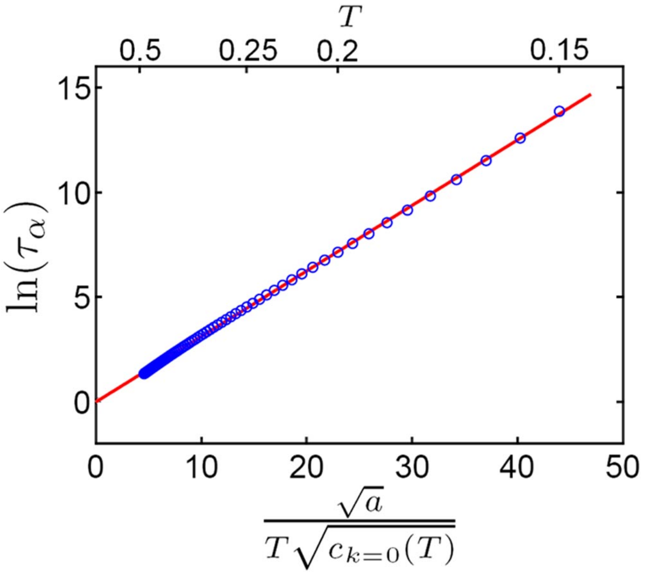

FIG. 5 (color online). Comparison of the measured spin rotational relaxation times τ_α (points) with the relaxation time predicted by Eq. (10) (continuous line).

state with antiferromagnetic order. Thus, the offered statistical mechanics explains very well the phenomenology of this system. Note that both of these transitions refer to finite systems, where sufficiently small concentrations mean effectively zero concentration.

The greatest challenge for the statistical mechanics is whether it can also predict the measured relaxation times. Jamming is caused by the rapid reduction in the mol fraction of some spin configurations, leading to a loss of ergodicity. To see this, consider the quasiparticles with $k = 0$. These are the highest in energy, and, accordingly, their mol fraction goes to zero first when the temperature cools down. Using then the mol fraction $c_{k=0}$ in comparison with the area per particle $a = A/N$, we form a length scale ξ according to

$$\xi(T) \equiv \sqrt{a/c_{k=0}(T)}. \tag{9}$$

When $c_{k=0} \rightarrow 0$, the length scale $\xi \rightarrow \infty$, defining regions of increasing size that are jammed and therefore contributing to an increasing relaxation time. Spin relaxations are dominated by correlated stringy (one-dimensional) chains, and we estimate the number of quasiparticles involved N^* as $N^*(T) \approx \xi(T)$. The relaxation time is determined by the free energy barrier, and, denoting by μ the chemical potential per quasiparticle, we write [5,8]

$$\tau_\alpha = \tau_0 \exp\left[\frac{N^*(T)\mu}{T}\right] = \tau_0 \exp\left[\frac{\mu\sqrt{a}}{T\sqrt{c_{k=0}(T)}}\right]. \tag{10}$$

Note that this prediction differs essentially from the Adam-Gibbs formula [9] in the sense that it does not predict a divergent τ_α at any finite temperature but rather an enormous increase in τ_α when $c_{k=0} \rightarrow 0$ exponentially fast. The statistical mechanics does not allow $c_{k=0} = 0$. Of course, in any finite system "exponentially small" mol fractions can be actually zero, and the relaxation time can be effectively infinite. The theory does not recognize, however, a sharp transition in the thermodynamic limit.

The comparison of the prediction (10) to the measured values of the relaxation times (measured as explained from the rotational autocorrelation functions [2]) is shown in Fig. 5. We note both the excellent agreement and the fact that τ_0 is of the order of unity, as expected in the limit $T \rightarrow \infty$, where the relaxation time should be the particle vibration time. We again draw the attention of the reader to Fig. 3 in Ref. [5], where a fit to the relaxation time is achieved, using similar ideas. In the problem there, the relaxation was configurational rather than via an internal variable as here, and typically relaxation events spanned two-dimensional correlated domains, making the free energy barrier proportional to ξ^2. The equal usefulness of the ideas used, with the only change being the identification of the quasispecies, their degeneracy and the constraints on the statistical mechanics give us hope that the approach is quite general and can be applied to glass-forming systems of a very different nature. Whether or not such a computer-assisted statistical mechanics can be applied to three-dimensional glass formers is a question that must await future research.

This work had been supported in part by the German–Israeli Foundation, the Minerva Foundation, Munich, Germany, and the Israel Science Foundation.

[1] See, for example, Ya. E. Ryabov, Y. Hayashi, A. Gutina, and Y. Feldman, Phys. Rev. B **67**, 132202 (2003), and references therein.
[2] H. Shintani and H. Tanaka, Nature Phys. **2**, 200 (2006).
[3] D. Deng, A. S. Argon, and S. Yip, Phil. Trans. R. Soc. A **329**, 549 (1989).
[4] D. N. Perera and P. Harrowell, Phys. Rev. E **59**, 5721 (1999), and references therein.
[5] E. Aharonov, E. Bouchbinder, H. G. E. Hentschel, V. Ilyin, N. Makedonska, I. Procaccia, and N. Schupper, Europhys. Lett. **77**, 56 002 (2007).
[6] H. G. E. Hentschel, V. Ilyin, N. Makedonska, I. Procaccia, and N. Schupper, Phys. Rev. E **75**, 050404(R) (2007).
[7] M. P. Allen and D. J. Tieldesley, *Computer Simulations of Liquids* (Clarendon, Oxford, 1991).
[8] J. P. Bouchaud and G. Biroli, J. Chem. Phys. **121**, 7347 (2004).
[9] G. Adam and J. H. Gibbs, J. Chem. Phys. **43**, 139 (1965).